Volume 1 | Number 1 | Jan 2013 | Pages 1–100

Journal of
Materials Chemistry A

Materials for energy and sustainability
www.rsc.org/materialsA

ROYAL SOCIETY OF CHEMISTRY

ROYAL SOCIETY OF CHEMISTRY

www.rsc.org/materialsA

Journal Name

COMMUNICATION

Facile, continuous and large-scale synthesis of CL-20/HMX nano co-crystals with high-performance by ultrasonic spray-assisted electrostatic adsorption method

Bing Gao,[a‡] Dunju Wang,[b‡] Juan Zhang,[a] Yingjie Hu,[c] Jinpeng Shen,[a] Jun Wang,[a] Bing Huang,[a] Zhiqiang Qiao,[a] Hui Huang,[a] Fude Nie[*a] and Guangcheng Yang[*a]

High-performance of CL-20/HMX nano co-crystals is readily synthesized by ultrasonic spray-assisted electrostatic adsorption method. This facile and continuous approach reduces handling time, minimizes the potential of aggregation via the electrostatic repulsive force among nano cocrystal particles and opens up new perspectives in fabricating various organic nano-sized co-crystals on a large-scale.

High-performance i.e., higher density, faster detonation velocity, good thermal stability, and desensitization or reduction of the sensitivity of energetic materials (EMs) have been an ideal target and essential subject of interest since their discovery.[1] Research efforts have been devoted to tailor and improve EMs properties by adjusting substance compositions, controlling material morphology,[2] reducing particle size,[3] and synthesizing new materials.[4] Co-crystals have demonstrated great potentials in various important applications by adjusting their crystal structure at the molecular level in the field of material science.[5-8] By virtue of co-crystallization technology, the physico-chemical properties of two independent components can be efficiently combined. This strategy has been widely used to develop organic non-linear optics[9] and organic optoelectronic materials.[10] In the field of energetic materials (EMs), including explosives, propellants, and pyrotechnics, has been a tremendously benefited from this strategy by successfully improving the performance of the density, stability, friction, and shock sensitivity in the form of co-crystals, based on previous studies on novel 1,3,5,7-tetranitro-1,3,5,7-tetrazocane (HMX)/1,3,5-triamino-2,4,6-trinitro-benzene (TATB), CL-20/benzotrifuroxan (BTF), CL-20/2,4,6-trinitrotoluene (TNT), energetic co-crystals,[11] and previous reports that were published.[4, 12]

On the other hand, materials under nanoscale often exhibit unique physico-chemical properties because of their small-size effect and large specific surface area. The preparation of nanomaterials has become a remarkable and indispensable technique in science and technology. A series of nano-sized explosives, such as HMX, TATB, 3-nitro-1,2,4-triazole-5-one (NTO), 1,1-diamino-2,2-dinitroethene (FOX-7), and CL-20,[3, 13] have been successfully prepared. They have important functions in weapon system, micro/nano thruster, booster, and MEMS.[14] Although new EMs are being fabricated, the limitation in their combination property has restricted their

implementation. Thus, the integration of nanotechnology and co-crystallization provids a new strategy to develop novel high-performance EMs. Nano co-crystals of the magnetic and pharmaceutical[15] that have been previously synthesized demonstrated outstanding physical and chemical properties. However, reports on nano energetic co-crystals in the field of EMs are not available to date.

HMX is an explosive that is well-known since 1949.[16] HMX has a higher explosive power and density than 1,3,5-trinitro-1,3,5-triaziane (RDX).[17] CL-20 is another novel explosive, which is also known as HNIW.[18] This explosive exhibits the highest density and is a caged nitramine explosive that can be used as a component in propellant formulations. While, The high mechanical sensitivity limits the further application of these compounds in the military field. CL-20/HMX co-crystals with high power explosive and good sensitivity that has been previously prepared exhibited higher combination property than CL-20/RDX and other energetic co-crystals which offers high explosive power and oxygen balance than β-HMX, and exhibits a similar sensitivity to that of HMX by Matzger group.[10]

Despite their success in improving materials properties, energetic co-crystals prepared by conventional methods can not achieve more demands for further application. Thus, the promising way of how to synthesize energetic co-crystals with superior performances is raised.

In this paper，we offers a facle and continuous approach to synthesize nano-sized energetic co-crystals with a narrow particle size (50 nm) and size distribution by the method (See Scheme 1). The nano-sized co-crystals was synthesized from CL-20 and HMX (Scheme 1a) with a 2:1 molar ratio. Besides desensitization properties that has been proved,[12] the obtained CL-20/HMX nono cocrystals show a detonation velocity of 9500 m s^{-1} and the density is 1.945 g cm^{-3} at room temperature and high to 2.006 g cm^{-3} at 0 K. The cocrystal CL-20/HMX exhibits high energy-release efficiency and excellent thermal stability, it only has a unique exothermic peak at 243.5 °C which approximately shifts lower 40 °C than β-HMX. In addition, This technique (Scheme 1c, Fig.S1 ESI†) avoids the post treatment of products such as drying, filtering, and evaporation, reduces handling time, minimizes the potential of aggregation via the electrostatic repulsive force among nano cocrystal particles and

opens up new perspectives on large-scale synthesis of other organic nano cocrystal materials.
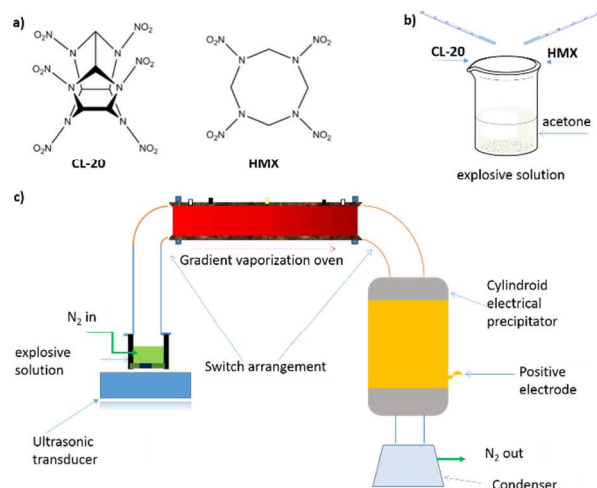
Scheme 1 (a) Chemical structures of 2,4,6,8,10,12-hexanitro-2,4,6,8,10,12-hexaazaisowurtzitane(CL-20) and 1,3,5,7-tetranitro-1,3,5,7-tetrazacyclooctane (HMX), (b) two explosives that were dissolved in acetone at 298 K, and (c) brief representation of the apparatus for nano co-crystals via the ultrasonic spray-assisted electrostatic adsorption (USEA) method.

The co-crystal CL-20/HMX structure was distinguished from raw CL-20 and HMX via powder X-ray diffraction (PXRD). Fig. 1 shows the PXRD pattern, wherein the three most intense peaks of raw HMX and CL-20 at 2θ = 31.9º, 14.67º, and 29.55º, and those at 2θ=12.52º, 30.36º, and 13.86º, respectively, were absent. Comparison of the co-crystal patterns revealed peaks at 2θ = 13.2º, 29.7º, and 28.0º, which were consistent with co-crystal formation.[12] HMX existed in chair conformation, which was regarded as β-HMX, this substance is the densest and most stable form of the raw material. Several HMX co-crystals that have been recently synthesized also produced this type of conformation.[12, 19] CL-20 was present in the high-density β and γ polymorph of the co-crystal CL-20/HMX (Fig. S2 and Tab. S1, ESI†), as confirmed via Raman
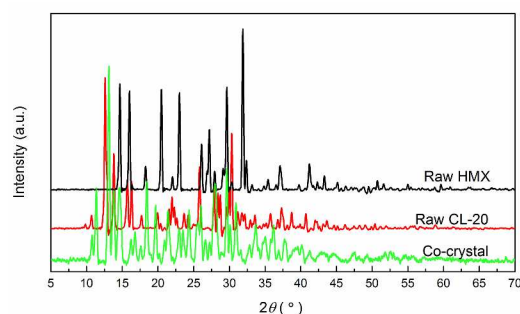
spectroscopy.

Fig. 1 Comparison of the PXRD patterns of raw HMX, raw CL-20, and nano-sized co-crystals via ultrasonic spray-assisted electrostatic adsorption (USEA) method.

The difference between both raw explosives was observed based on the Raman spectra of the co-crystal (Fig. 2). PXRD results and Raman spectroscopy (Fig. S3 and Tab. S2, ESI†) were used to

determine the co-crystal compound. The structure of the co-crystal is also presented which is the same as former published[12] (Tab. S3, ESI

†)
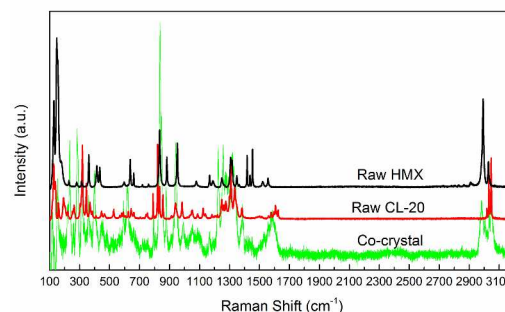
Fig. 2 Comparison of the Raman spectra of raw HMX, raw CL-20, and nano-sized CL-20/HMX co-crystals.

The nano-sized co-crystal particles that were obtained via the USEA method were characterized via FE-SEM (Fig. 3). Fig. 3c shows the spheroidic morphology of majority of the co-crystals particles that were formed (Figs. 3d and e) compared with raw CL-20 (Fig. 3a) and raw HMX (Fig. 3b). The average particle size was 253 ± 30 nm, which was calculated from the sizes of more than 300 particles from the SEM images (Fig. 3c), this method was performed using the statistics of the Smileview software. The DLS result revealed that the particle size distribution was relatively narrow with small sizes from 50 nm to 400 nm (Fig. S4, ESI†).
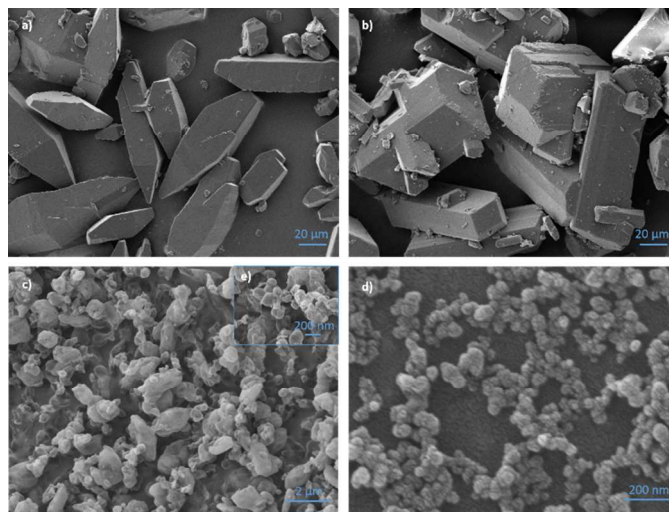
Fig. 3 FE-SEM micrographs of raw and prepared co-crystals: (a) raw CL-20, (b) raw HMX, (c) nano-sized co-crystal CL-20/HMX prepared via ultrasonic spray-assisted electrostatic adsorption (USEA) method, (e) partial magnification of the co-crystal CL-20/HMX from (c), and (d) after ultrasound at 40 kHz for 30 min.

Well-distributed spheroidic particles of approximately 50 nm were produced (Fig. 3d) via ultrasonic treatment at 40 kHz for 30 min. The powder and supersonic frequency employed must be below a specific value to obtain a stable co-crystal structure. More than 20 min of treatment time was necessary to produce well-distributed particles. No obviously particle aggregation was observed in the SEM micrographs of the samples prepared via the USEA method. This occurrence was due to the disordered and complex aerosol size distribution, which was generated by a piezoelectric transducer

during aerosol production. As such, a difference was observed in the aerosol size and its distribution.[20] Small aerosol size droplets that contained the molecules of the two explosives crystallized the small particles during crystallization. Repulsive forces that existed in each particle in the electrostatic field reduced the crystals' agglomeration effect. The airflow effect of high-purity nitrogen (N_2, > 99.999%) decreased the droplet size to a particular extent. A fast gas flow rate facilitated the synthesis of the nano-sized co-crystal. A timely crystal delivery decreased the crystallization period. Solvent rupture (acetone) at high temperatures (above boiling point) and fast evaporation from the droplets accelerated the crystal growth. Nanoscale co-crystals were produced by balancing crystal growth and motivational speed under an electrostatic field force.

Density is one of the most important combination properties in the practical application of EMs. The co-crystal CL-20/HMX produced in this study had a theoretical density of 2.006 ± 1 g cm^{-3}
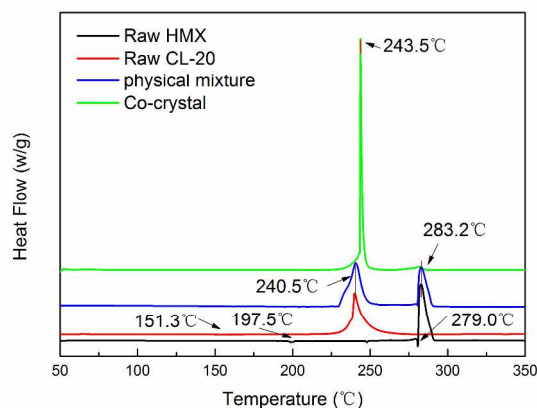
Fig. 4 DSC curves of pure HMX, pure CL-20, and a mixture of the two explosives and nano-sized co-crystal CL-20/HMX (heating rate: 10 °C min $^{-1}$).

at 0 K, and 1.945 g cm^{-3} at room temperature which is only lower than that ε-CL-20 with those all pure forms (1.950 cm^{-3} to 2.044 cm^{-3})[21] but is higher than that of the most stable and densest β-HMX (1.890 cm^{-3}).[22] The detonation velocity, which is the major detonation property of Ems, was measured using the following equation:[23]

$$D = A\varphi^{1/2}(1 + B\rho_0) \quad (1)$$

$$\varphi = NM^{1/2}Q^{1/2} \quad (2)$$

where A=1.01, B=1.30; ρ_0 is the density of the explosive (g cm^{-3}); and D is the detonation velocity of the explosive (km s^{-1}); N is the number of moles of gaseous detonation products (per gram)of explosive, M is the average weight of these gases; Q is the chemical energy of the detonation reaction($-\Delta H_0$ per gram), and ρ_0 is the initial density. The detonation velocity of the nano-sized cocrystal CL-20/HMX (about 9480 m s^{-1}) was similar with that of pure CL-20 (9600 m s^{-1}) but higher than that of pure HMX explosive (9100 m s^{-1}).

The thermal properties of nano-sized co-crystal CL-20/HMX made it chemical stable EMs (Fig. 4). Pure HMX was converted to δ-HMX at temperatures above 197.5 °C and had a melting temperature of 279.0 °C below decomposition. This result was due to the fracture of C skeleton in an HMX molecule.[24] A change in conformation was also observed in pure CL-20 at a phase transition

temperature of 151.3 °C (ε-γ phase transition).[25] No phase change was observed in the nano-sized co-crystal C/H, the co-crystal form structure was not destroyed until 243.5 °C (at a heating rate of 10 °C min^{-1}). The peak shifted left with a decrease by 40 °C for pure HMX, which was close to the decomposition peak of CL-20 (240.5 °C). The unique thermal behaviour of the co-crystal, which was different from the physical mixture of the two explosives that depended on the molecular structure of the co-crystal form, was caused by an increase in the ratio of the surface and interior atoms compared with that of the pure explosives. This occurrence led to a higher surface energy and the shifting of the decomposition peak (almost decreased with decreasing nanomaterial particle size). The decomposition of the nano-sized co-crystal was determined within a narrow temperature range (234.6 °C to 250.7 °C) compared with that of pure CL-20 (227.6 °C to 269.3 °C), and near that of pure HMX (280.3 °C to 291.8 °C), which meant that they possessed high energy release efficiency. Table 1 shows the thermal behaviour comparison of the three solid-state explosives.

Table 1 Thermal analysis and thermal performance of the pure explosives and prepared nano-sized co-crystal CL-20/HMX.

Entry	APS (μm)[a]	SD (μm)[b]	T_1 (℃)[c]	T_2 (℃)[d]	T_3 (℃)[e]
Pure HMX	15	> 20	197.5	279.0	283.2
Pure CL-20	10	> 20	151.3	/	240.5
Nano co-crystals	0.25	0.05-0.4	/	/	243.5

[a] Average particle sizes. [b] Size distribution. [c] The phase-transition temperature. [d] Melting temperature. [e] Exothermal decomposition peak.
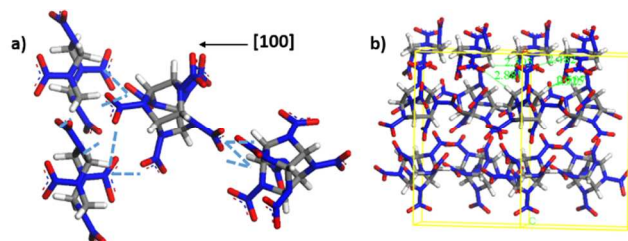
Fig. 5 Intermolecular hydrogen bond distances in the co-crystal C/H structure: (a) Nitro–hydrogen and nitro–nitro interactions between CL-20 and HMX molecules (dashed line) in the **[100]** direction. b) Bulk crystal structure of co-crystal C/H with H bonding interactions between the C-H and nitro groups of CL-20 and HMX in co-crystal form.

In the co-crystal CL-20/HMX form, the co-crystal structure is exclusively defined by H bonding interactions between the C-H and nitro groups among the CL-20 molecules; the same H bonding interactions of CL-20 appeared in pairs and HMX in the co-crystal form (Fig 5a) in the **[100]** direction. With the help of the weak (compared with the chemical bond) but vital OH···O contact (hydrogen bond length: 1.925 Å, 2.305 Å, 2.482 Å, 2.507 Å, and 2.881 Å), the repeated growth of explosive molecules was observed with a periodicity on scale in the space lattice. Finally, a three-dimensional structure (Fig 5b) was formed, and nano-sized crystals were developed.

Considering the intermolecular hydrogen-bond interactions, a model of CL-20 and HMX in a 2:1 molar ratio was constructed to study the co-crystal structure at periodic boundary conditions. In this study, DFT calculations using GGA-PBE[26] functional were performed using the Materials Studio Dmol³ software from Accelrys.[27] The basis sets were DNP and effective core potentials. The real space cutoff radius was 0.37 nm. The convergence tolerance

for SCF was 1.0×10^{-5} Ha. Geometry optimization for energy and maximum force were 2.0×10^{-5} Ha and 0.004 Ha/Å, respectively.

Fig. 6 shows all possible intermolecular H bond distances in the co-crystal CL-20/HMX structure and H bond interactions between nitro groups and adjacent H atoms. The intermolecular forces were strong enough to maintain structural stability of the crystal to a particular degree and can reduce the friction and shock sensitivity between themselves with the help of particle size reduction, this result has been reported in previous studies.[2, 28] of course, besides this, the sensitivity is highly correlated with the particle size, synthesis and crystallization method and so on.[29]
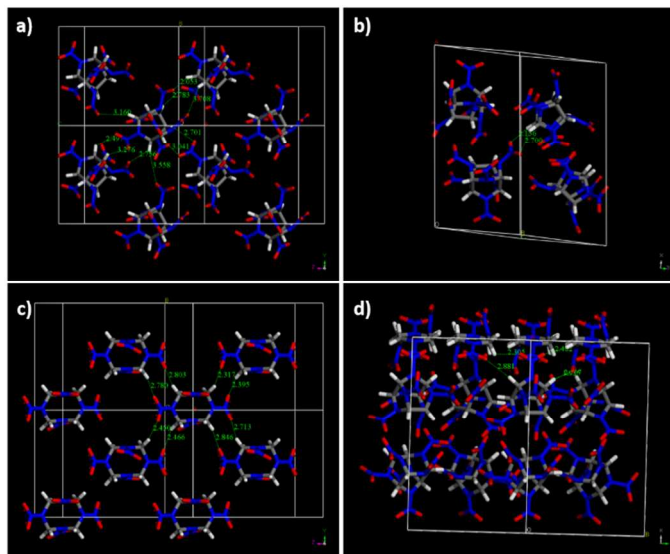
Fig. 6 H bonding analysis of the co-crystal CL-20/HMX (a) H bonding interactions between C-H and nitro groups in the same layer of CL-20 molecules (b) adjoining H bonding interactions of CL-20
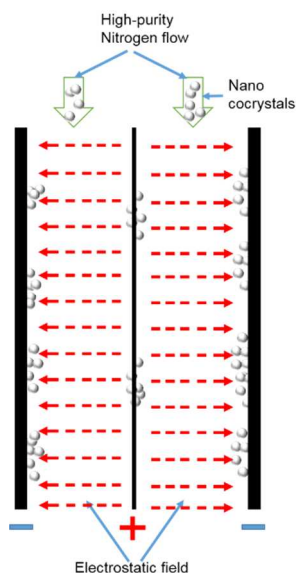
appearing in pairs (c) and H bonding interactions of HMX of the co-crystal CL-20/HMX (d).

Fig. 7 The repulsive forces existing among particles and collection of nano cocrystals in cylindroid electrical precipitator.

All of these intermolecular hydrogen bonding interactions (Fig. S5 and Tab. S4, ESI†) were similar to those of the CL-20/TNT co-crystal and shorter than similar H bonds that exist in pure CL-20 and HMX crystals. The co-crystal structure was stabilized by a number of C-H hydrogen bonds, each involving nitro group oxygen atoms.

Specially, When nano cocrystal particles were flowed into cylindroid electrical precipitator as shown in Fig. 7, particles were positively charged and thus separated naturally due to the electrostatic repulsive forces. With the synergistic action of each other, nano cocrystal particles without agglomeration effect were obtained directly without further follow-up treatment i.e., drying, filtering, and evaporation.

Top-down methods exhibit an intrinsic inability to produce organic nano cocrystals smaller than 100 nm, which was mainly due to ductility and ease of losing crystallinity.[30] Difficulty in synthesizing several particles was also observed. The inevitable impact and friction caused by the reduction of products would also occur in the extra treatment, especially for EMs. Thus, we developed this novel bottom-up approach without follow-up treatment which is really necessary to facilitate the production of crystalline particles with sizes of a few hundred nanometers. As expected, by varying the organic solute, reaction temperature and electrostatic voltage, various nano cocrystals CL-20/NTO (Fig. S6 and Fig. S7, ESI†) and CL-20/1,3-dinitrobenzene (DNB) *etc*. with different sizes can be prepared by the USEA method, due to the same mechanisms of fast evaporation and limited crystallization.

Conclusions

In conclusion, we performed a facile, large-scale synthesis of an energetic nanoscale cocrystal composed of a 2:1 molar ratio of CL-20 and HMX via the USEA method. The mean particle size was 50 nm, and the particle size distribution was relatively narrow. The cocrystal produced was stable because of a number of C-H hydrogen bonds, each involving nitro group oxygen atoms. The density of the nano-sized CL-20/HMX co-crystal was 1.945g cm^{-3} and high to 2.006 g cm^{-3} at 0 K. Its detonation velocity was 9480 m s^{-1}, which was higher than that of pure HMX explosive and comparable with that of pure CL-20. The cocrystal CL-20/HMX exhibited high energy-release efficiency and a unique exothermic peak at 243.5 °C. The peak shifts left by 40 °C compared to that of pure HMX. This strategy not only combined the advantages of cocrystals and nano effects but also opens up new perspectives and advances development in the science and technology of organic cocrystal materials. The method may be employed in industrial production on a large-scale for preparing high-performance materials with excellent properties.

Acknowledgements

Notes and references

[a] Institute of Chemical Materials, China Academy of Engineering Physics (CAEP), Mianyang 621900, PR China

[b] School of National Defence science and Engineering, Southwest University of Science and Technology (SWUST), Mianyang 621900, China

[c] School of Biochemical and Environmental Engineering, Nanjing Xiaozhuang University, Nanjing 211171, China

‡These authors contributed equally to this work.

Experimental Details

Materials and methods

CL-20 (20 to 80 μm) was provided by Liaoning Qing Yang Chemical Industry Co., Ltd, China. HMX (20 to 70 μm) NTO and DNB was obtained from East Chemical Industry Company, China. Other chemicals and reagents (AR grade) that were used in this study were trade-purchased and used without further purification.

Nano cocrystal synthesis

Raw CL-20 and HMX were dissolved in 50.0 mL of acetone (solvent, Scheme 1b) at a concentration below saturation point at 25 °C. The resulting explosive solution was placed in a 250 mL ultrasonic container, wherein aerosols were produced on the solution's upper portion when the ultrasonic transducer was turned on. The aerosols were converted to droplets and were transported by an inert gas (high-purity N_2 at 60 mL min^{-1}) towards an (oven which has different temperatures in different zones. When droplets enter the oven, the solvent evaporates and nano-sized co-crystals were formed. The nano co-crystals moved out of the oven with the help of the gas and were dried at 60±1 °C (higher than the boiling point of acetone). Nano cocrystals were adsorbed via directional movement from an anode to a cathode under electrostatic force attraction (electric tension: 0–5 kV). The particles mainly accumulated near the bottom of the precipitator. Samples that were obtained from the bottom of the precipitator were used without further treatment such as drying, filtering, and evaporation.

PXRD data were obtained via X-ray diffraction (XRD, X'Pert Pro, PANalytical, Netherlands). The particle size and its distribution were calculated by counting more than 300 particles from the obtained SEM images via the statistics of the Smileview software. The morphological information of the samples is characterized via field emission scanning electron microscopy (FE-SEM, Ultra-55, Carl Zeiss, Germany) operated at an acceleration voltage of 5 kV. The samples are sputtering coated with gold in vacuum at 6 $^{-10}$ Pa for 50 s before imaging. The thermal properties of the samples were analysed using a differential scanning calorimeter (DSC, PerkinElmer Diamond, America). The operational conditions employed were as follows: sample mass 3.00 mg, heating rate 10 °C min-1, N_2 flow rate 30 mL min^{-1}.

1 (a) A. Sikder, N. Sikder, *J. Hazard. Mater.,* **2004**, *112*, 1-15; (b) M.-J. Crawford, T. M. Klapötke, J. Welch, *Angew. Chem. Int. Ed.,* **2005**, *44*, 1909-1909; (c) Q. Wu, W. Zhu and H. Xiao *J. Mater. Chem., A* 2014,*2*, 13006-13015

2 H. Cai, L. Tian, B. Huang, G. Yang, D. Guan, H. Huang, *Micropor. Mesopor. Mat.,* **2013**, *170*, 20-25.

3 a) G. Majano, S. Mintova, T. Bein, T. M. Klapötke, *Adv. Mater.,* **2006**, *18*, 2440-2443; b) G. Yang, F. Nie, H. Huang, L. Zhao, W. Pang, *Propellants, Explos., Pyrotech.,* **2006**, *31*, 390-394; c) G. Yang, F. Nie, J. Li, Q. Guo, Z. Qiao, *J. Energ. Mater.,* **2007**, *25*, 35-47.

4 O. Bolton, A. J. Matzger, *Angew. Chem. Int. Ed.,* **2011**, *50*, 8960-8963.

5 a) J. R. Sander, D. K. Bucar, R. F. Henry, G. G. Zhang, L. R. MacGillivray, *Angew. Chem. Int. Ed.,* **2010**, *49*, 7284-7288;b) Ö. Almarsson, M. J. Zaworotko, *Chem. Commun.* **2004**, 1889-1896.

6 D. J. Berry, C. C. Seaton, W. Clegg, R. W. Harrington, S. J. Coles, P. N. Horton, M. B. Hursthouse, R. Storey, W. Jones, T. Friscic, *Cryst. Growth. Des.,* **2008**, *8*, 1697-1712.

7 M. Khan, V. Enkelmann, G. Brunklaus, *J. Am. Chem. Soc.* **2010**, *132*, 5254-5263.

8 M. L. Brader, M. Sukumar, A. H. Pekar, D. S. McClellan, R. E. Chance, D. B. Flora, A. L. Cox, L. Irwin, S. R. Myers, *Nat. Biotechnol.* **2002**, *20*, 800-804.

9 a) C. Bosshard, M. S. Wong, F. Pan, P. Günter, V. Gramlich, *Adv. Mater.,* **1997**, *9*, 554-557; b) J. Yu, Y. Cui, C. Wu, Y. Yang, Z. Wang, M. O'Keeffe, B. Chen, G. Qian, *Angew. Chem. Int. Ed.,* **2012**, *51*, 10542-10545; c) J. Chen, M. Badioli, P. Alonso-Gonzalez, S. Thongrattanasiri, F. Huth, J. Osmond, M. Spasenovic, A. Centeno, A. Pesquera, P. Godignon, A. Z. Elorza, N. Camara, F. J. Garcia de Abajo, R. Hillenbrand, F. H. Koppens, *Cah. Rev., The* **2012**, *487*, 77-81.

10 a) D. Yan, A. Delori, G. O. Lloyd, T. Friscic, G. M. Day, W. Jones, J. Lu, M. Wei, D. G. Evans, X. Duan, *Angew. Chem. Int. Ed.,* **2011**, *50*, 12483-12486; b) A. De Girolamo Del Mauro, M. Carotenuto, V. Venditto, V. Petraccone, M. Scoponi, G. Guerra, *Chem. Mater.,* **2007**, *19*, 6041-6046; c) T. Schiros, G. Kladnik, D. Prezzi, A. Ferretti, G. Olivieri, A. Cossaro, L. Floreano, A. Verdini, C. Schenck, M. Cox, A. A. Gorodetsky, K. Plunkett, D. Delongchamp, C. Nuckolls, A. Morgante, D. Cvetko, I. Kymissis, *Adv. Energy. Mater.* **2013**, *3*, 894-902.

11 a) P. Shen, X. H. Duan, Q. P. Luo, Y. Zhou, Q. Bao, Y. J. Ma, C. H. Pei, *Cryst. Growth. Des.,* **2011**, *11*, 1759-1765; b) Thottempudi, J. M. Shreeve, *J. Am. Chem. Soc.,* **2011**, *133*, 19982-19992.

12. a) O. Bolton, L. R. Simke, P. F. Pagoria, A. J. Matzger, *Cryst. Growth. Des.,* **2012**, *12*, 4311-4314; b) D. I. A. Millar, H. E. Maynard-Casely, D. R. Allan, A. S. Cumming, A. R. Lennie, A. J. Mackay, I. D. H. Oswald, C. C. Tang, C. R. Pulham, *Cryst. Eng .Comm.,* **2012**, *14*, 3742.

13 a) Bayat, M. Zarandi, M. A. Zarei, R. Soleyman. *J. Mol. Liq*., **2014**. 193, 83-86; b) Yu, H. Ren, X. Y. Guo, X. B. Jiang, Q. J. Jiao. *J. Therm. Anal. Calorim*., **2014**. 117, 1187-1199; c) Yang, H. Li, X. Zhou, C. Zhang, H. Huang, J. Li, F. Nie, *Cryst. Growth. Des.,* **2012**, *12*, 5155-5158; d) Yang, H. Li, H. Huang, X. Zhou, J. Li, F. Nie, *Propellants, Explo. Pyrotech.,* **2013**, *38*, 495-501; e) Zhang, C. Guo, X. Wang, J. Xu, X. He, Y. Liu, X. Liu, H. Huang, J. Sun, *Cryst. Growth. Des.,* **2013**, *13*, 679-687.

14 a) Talawar, R. Sivabalan, T. Mukundan, H. Muthurajan, A. Sikder, B. Gandhe, A. S. Rao, *J. Hazard. Mater.,* **2009**, *161*, 589-607; b) Fuchs, D. Stec Iii, **2007**, *6556*, 65561B-65561B-65512; c) Losic, J. G. Mitchell, N. H. Voelcker, *Adv. Mater.,* **2009**, *21*, 2947-2958.

15 a) R. Sander, D. K. Bucar, J. Baltrusaitis, L. R. MacGillivray, *J. Am. Chem. Soc.,* **2012**, *134*, 6900-6903; b) K. Bucar, L. R. MacGillivray, *J. Am. Chem. Soc.,* **2007**, *129*, 32-33; c) C. Karunatilaka, D. K. Bucar, L. R. Ditzler, T. Friscic, D. C. Swenson, L. R. MacGillivray, A. V. Tivanski, *Angew. Chem.,* **2011**, *50*, 8642-8646.

16 W. Bachmann and J. Sheehan, *J. Am. Chem. Soc.*, 1949, **71**, 1812.

17 (a) R. GrahamáCooks, *Chem.l Comm*, 2007, 2142-2144; (b) A. E. van der Heijden and R. H. Bouma, *Crys. growth. des.*, 2004, **4**, 999-1007.

18 A. T. Nielsen, R. A. Nissan, D. J. Vanderah, C. L. Coon, R. D. Gilardi, C. F. George and J. Flippen-Anderson, *J. Org. Chem.*, 1990, **55**, 1459-1466.

19 a) Ordzhonikidze, A. Pivkina, Y. Frolov, N. Muravyev, K. Monogarov, *J. Therm. Anal. Calorim.* **2011**, *105*, 529-534; b) C. Achuthan, C. Jose, *Propellants, Explo. Pyrotech.,* **1990**, *15*, 271-275; c) K. B. Landenberger, A. J. Matzger, *Cryst. Growth. Des.,* **2012**, *12*, 3603-3609.

20 R. Rajan, A. Pandit, *Ultrasonics,* **2001**, *39*, 235-255.

21 a) Kholod, S. Okovytyy, G. Kuramshina, M. Qasim, L. Gorb, J. Leszczynski, *J. Mol. Struct.* **2007**, *843*, 14-25; b) Nair, R. Sivabalan, G. Gore, M. Geetha, S. Asthana, H. Singh, *Combust. Explo. Shock. Waves.,* **2005**, *41*, 121-132.

22 a) Simpson, P. Urtiew, D. Ornellas, G. Moody, K. Scribner, D. Hoffman, *Propellants, Explo. Pyrotech.,* **1997**, *22*, 249-255; b) L. Cui, G.-F. Ji, X.-R. Chen, Q.-M. Zhang, D.-Q. Wei, F. Zhao, *J. Chem. Eng., Data* **2010**, *55*, 3121-3129.

23 M. J. Kamlet and S. Jacobs, *J. chem. Phys.*, 1968, **48**, 23-35.

24 a) Ordzhonikidze, A. Pivkina, Y. Frolov, N. Muravyev, K. Monogarov, *J. Therm. Anal. Calorim.* **2011**, *105*, 529-534; b) C. Achuthan, C. Jose, *Propellants, Explo. Pyrotech.,* **1990**, *15*, 271-275.

25 R. Turcotte, M. Vachon, Q. S. M. Kwok, R. Wang, D. E. G. Jones, *Thermochim, Acta.,* **2005**, *433*, 105-115.

26 J. P. Perdew, K. Burke, M. Ernzerhof, *Phys. Rev. Lett.* **1996**, *77*, 3865.

27 B. Delley, *J. Chem. Phys.,* **2000**, *113*, 7756.

28 a) T, Sun, J. J. Xiao, Q. Liu, F. Zhao, H. Xiao. *J. Mater. Chem. A,* **2014**, 2, 13898–13904; b) C. Y. Zhang, Z. W. Yang, X. Q. Zhou, C. H. Zhang, Y. Ma,J. J. Xu, Q. Zhang, F. D. Nie, H. Z. Li. *Cryst. Growth. Des.,* **2014**, 14, 3923-3928.

29 a) J. Szczygielska, S. Chlebna, P. Maksimowski and W. Skupinski, *Cent. Euro. J. Energ. Mater.,* 2011, 8, 117-130; b) B. Tan, X. Long, R. Peng, H. Li, B. Jin and S. Chu, *J. phys. chem. A,* 2011, 115, 10610-10616; c) Y. Ma, A. Zhang, C. Zhang, D. Jiang, Y. Zhu and C. Zhang, *Cryst. Growth, Des.,* 2014, 14, 4703-4713.

30 a) F. Kesisoglou, S. Panmai, Y. Wu, *Adv Drug Deliver Rev* **2007**, *59*, 631-644; b) D. Horn, J. Rieger, *Angew. Chem. Int. Ed.,* **2001**, *40*, 4330-4361; c) T. J. Buschman, E. K. Miller, *Science,* **2007**, *315*, 1860-1862.

A table of contents entry

Graphic:
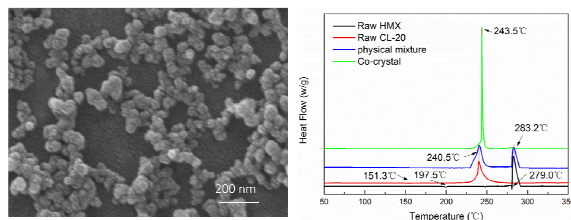
Text: Energetic CL-20/HMX nano cocrystals of about 50 nm with high-performance are synthesized by USEA method.